J Mater Sci: Mater Electron (2017) 28:14424–14429
DOI 10.1007/s10854-017-7303-x

Fabrication of Cu_2ZnSnS_4 thin films by simple solution method using citric acid as complexing agent

Hao Guan[1,2] · Honglie Shen[1] · Wei Wang[1]

Received: 9 March 2017 / Accepted: 5 June 2017 / Published online: 20 June 2017

Abstract Cu_2ZnSnS_4 (CZTS) films were prepared by sulfurizing Cu–Zn–Sn precursor deposited via a simple solution method using environment-friendly citric acid as complexing agent. A single Cu_2ZnSnS_4 thin film was obtained at 500 °C under a mixed N_2+H_2S (5%) atmosphere. The effects of sulfurization temperature on structural, morphological and optical properties were studied. The results showed that the CZTS thin film annealed at 500 °C exhibited large agglomeration of grains, ideal band gap ($E_g = 1.49$ eV) and high optical absorption coefficient ($>10^4$ cm^{-1}). The resulted carrier concentration and mobility were about 3.652×10^{18} cm^{-3} and 26.32 cm^2/Vs, respectively.

1 Introduction

Cu_2ZnSnS_4 (CZTS) has emerged as a most promising candidate for thin film solar cells with favorably matched band gap (1.1–1.5 eV) to solar spectrum and high optical absorption coefficient ($\geq10^4$ cm^{-1}), and it has been reported that the most efficient CZTS solar cells could reach 9.2% power conversion efficiency [1, 2]. Moreover, the elements of CZTS are earth-abundant and non-toxic elements [3]. So recent studies were extensively focused on CZTS thin film solar cells.

As for the synthesis method of CZTS thin films, a few techniques have been reported such as sputtering [4–7], spray pyrolysis deposition [8, 9], thermal evaporation [10], sol–gel [11, 12], electro-deposition [13–15], successive ionic layer adsorption and reaction (SILAR) [16–18], nanoparticle-based route [19, 20] and precursor-based route [21, 22]. Among these methods, the preparation of CZTS thin films by non-vacuum methods exhibit advantages owing to their simple and low cost equipments and the possibility for large-scale production.

As a cheap, safe and environment-friendly organic acid, citric acid (CA) arises much concern in synthesizing CZTS compounds. CZTS nanoparticles were prepared by a hydrothermal method using CA as surfactant [23]. Jin et al. reported a combusiton route for Cu–Zn–Sn–O precursor powder by using CA as organic fuel [24]. Jiang et al. synthesized CZTS thin film via a electrochemical deposition method using CA as orgainc additive [25]. To our knowledge, there are no reports about fabrication of CZTS thin film through a simple solution method by using CA as complexing agent. In this work, the CZTS thin films were prepared by sulfurizing Cu–Zn–Sn (CZT) precursors which were deposited by a simple solution method using water and citric acid (CA) as slovent and complexing agent, respectively, and the simple solution method was similar to the sol–gel method used for preparing CZTS thin films. Meanwhile, the limitation of large-scale production owing to amounts of environment-unfriendly and expensive solvent and stabilizer used in the sol–gel method can be overcome. It is recommended that the method is a simple and inexpensive one for preparing CZTS thin films.

✉ Honglie Shen
hlshenktz@163.com

[1] College of Materials Science and Technology, Nanjing University of Aeronautics and Astronautics, 29 Yudao Street, Nanjing 210016, People's Republic of China

[2] School of Materials Engineering, Yancheng Institute of Technology, 9 Yinbing Street, Yancheng 224051, People's Republic of China

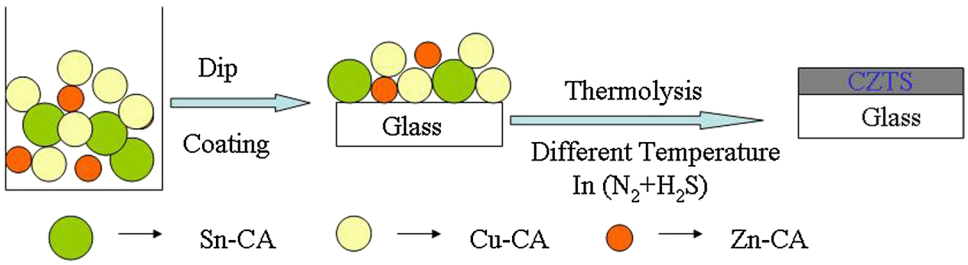

Fig. 1 Schematic diagram of sol–gel sulfurization process of CZTS thin films

Table 1 Chemical composition of CZTS thin films at different temperatures

Sulfurization temperature (°C)	Chemical composition (%)				Compositional ratio (%)			
	Cu	Zn	Sn	S	Cu/(Zn + Sn)	Cu/Sn	Zn/Sn	S/metal
400	26.84	12.69	12.59	49.88	1.06	2.1	1.01	0.99
450	26.59	13.01	11.34	49.06	1.09	2.3	1.15	0.96
500	26.5	13.05	11.24	49.21	1.09	2.4	1.16	0.97

2 Experimental details

2.1 Sample preparation

In this work, the main experiment process for the synthesis of CZTS thin film is shown in Fig. 1. For preparation of CZT precursors, $Cu(NO_3)_2$, $Zn(CH_3COO)_2$ and $SnCl_2$ in a mixture of 2, 1 and 1 mol/L were dissolved into the deionized water (40 ml) containing citric acid (molar ratio for ion of metal to citric acid is 1:3) and stirred for 10 min to obtain transparent solution. Citric acid was used as the complexing agent. To prepare thin films, the as-obtained complex ion solution was dip-coated onto the glass substrates followed by solvent-drying at 80 °C for 5 min. The coated substrates were annealed at different temperatures for 1 h in a tube furnace under a mixed $N_2 + H_2S$ (5%) atmosphere.

2.2 Sample characterization

X-ray diffraction (XRD) patterns were carried out using a *PANalytical X'Pert PRO* diffractometer with Cu K_α radiation ($\lambda = 0.15406$ nm). Raman spectra of the films were measured using a *JY-T64000* Raman spectrometer. Scanning electron microscopy (SEM) images were obtained using a *LEO-1530VP* scanning electron microscope. The optical characteristics were measured using a *Varian Cary 5000* spectrophotometer. The electrical properties were measured using a *ET-9000* electrical transport measurement.

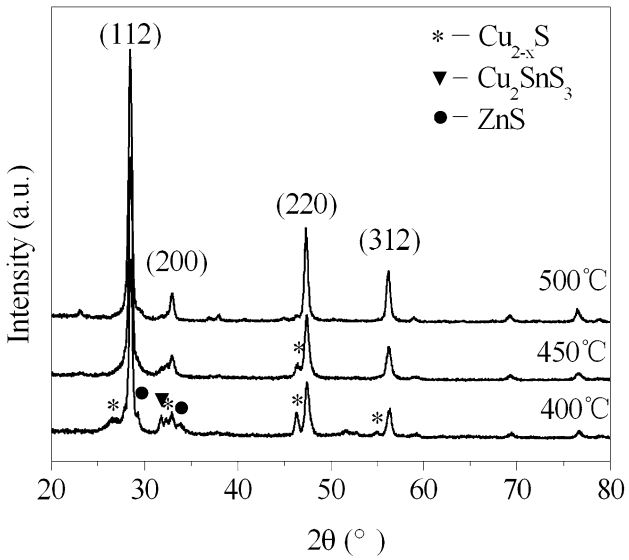

Fig. 2 XRD patterns of CZTS thin films at different temperatures

3 Results and discussion

3.1 Compositional analysis

The chemical composition and ratio of CZTS thin films measured by the energy dispersive X-ray spectroscopy are shown in Table 1. All CZTS thin films are in Cu-rich, Zn-rich and Sn-poor states. The [Cu]/[Sn] ratio in the thin films is 2.1, 2.3 and 2.4, respectively, which is related to the fact that the evaporation of Sn increases with increasing sulfurization temperature. For all thin films the ratio of sulfur to metal is around 1, indicating a complete sulfurization.

3.2 XRD characterization and Raman spectra

XRD patterns of CZTS thin films at different temperatures are shown in Fig. 2. It can be seen that the CZTS phase can be obtained over 400 °C. For the sulfurization temperature of 400 °C, some second phases such as $Cu_{2-x}S$, Cu_2SnS_3 and ZnS appear owing to inadequate reaction. There is also a $Cu_{2-x}S$ phase appeared in the XRD pattern when the sulfurization temperature rises to 450 °C, which cannot be confirmed by the Raman spectrum owing to its low content. A single CZTS phase can be obtained up to 500 °C. The diffraction peaks at $2\theta = 28.4°$, 32.9°, 47.3°, and 56.2° are associated to the (112), (200), (220) and (312) planes of kesterite Cu_2ZnSnS_4, respectively. The average grain sizes of as-obtained CZTS thin films at different temperatures can be calculated from the main (112) peaks by Debye–Scherrer formula. Based on θ, FWHM (β) and main crystallite size (D) of the related peaks, micro-strain (ε) and dislocation density (ρ) are further calculated. The corresponding formulas are given below [26, 27]:

$$\varepsilon = \frac{\beta cos\theta}{4} \quad (1)$$

$$\rho = \frac{1}{D^2} \quad (2)$$

Table 2 Estimated structural parameters of CZTS thin films at different temperatures

Sulfurization temperature (°C)	400	450	500
Grain size (nm)	12.7	14.9	17.1
Micro-stain (ε)$\times 10^{-2}$	16	13	11
Dislocation density (ρ)$\times 10^{15}$ (m^{-2})	6.2	4.5	3.4

The estimated values are shown in Table 2. The CZTS thin film at 500 °C shows the lowest micro-strain and dislocation density, while the largest grain size. From the XRD pattern of CZTS thin film at 500 °C, lattice parameters are calculated. The values of a and c are 5.424 and 10.848 Å, respectively. Comparing with standard bulk CZTS powder data from JCPDS 26-0575, $a = 5.427$ Å and $c = 10.84$ Å, relative shifts of 0.05 and 0.07% are obtained. It is indicated that the internal strain has no influence on the quality of the thin film, although it exists in the sample.

The crystallinity extent of the CZTS increases with increasing sulfurization temperature. The phenomenon is in accordance with the previous report [8]. The preparation of CZTS thin films can be explained as Fig. 3: firstly, the metal salts were dissloved in the deionized water containing citric acid, and the complex ion solution was obtained after aging some time. Secondly, the precursor films were dip-coated on glass substrates. Finally, the precursor films were annealed in a mixed $N_2 + H_2S$ (5%) atmosphere, and the CZTS thin films were obtained with the decomposition of citric acid.

Since the crystal structure of CZTS, Cu_2SnS_3 and β-ZnS are similar with each other [28], the phase structure of the annealed thin films was further investigated by Raman spectrum at room temperature. Figure 4 shows that the Raman spectra of the annealed thin films at different temperatures. The main Raman peak at about 336 cm^{-1} for the CZTS thin films annealed at 450 and 500 °C can be observed, whereas for the CZTS thin films at 400 °C there are two strong peaks at about 336 and 475 cm^{-1} corresponding to CZTS and $Cu_{2-x}S$ phases, respectively. In addition, the two weak shoulder peaks at about 267 and 273 cm^{-1} may be related to a small amount of cubic Cu_2SnS_3 and ZnS phases exist in the sample. Comparing with standard Raman peak at about 338 cm^{-1} for CZTS phase, the corresponding Raman

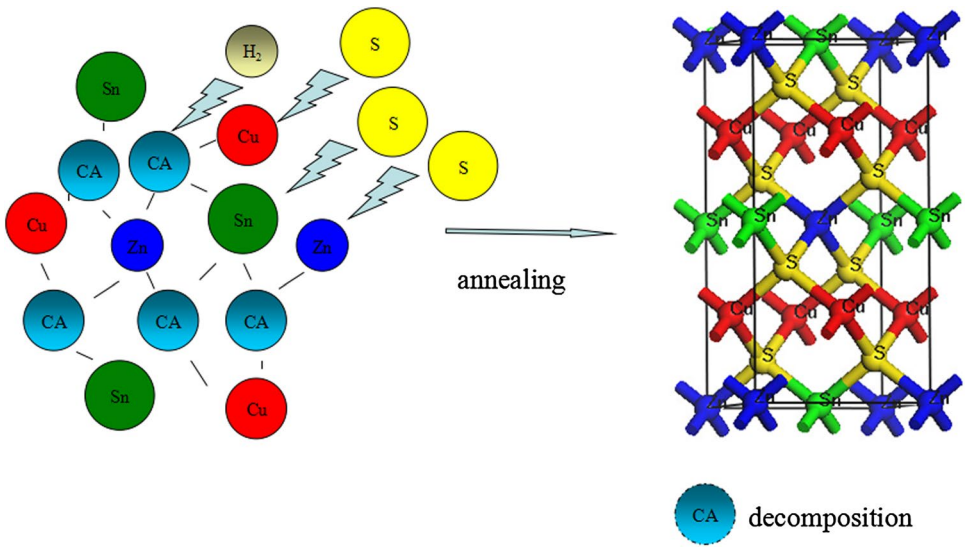

Fig. 3 Schematic illustration for the formation of CZTS thin films

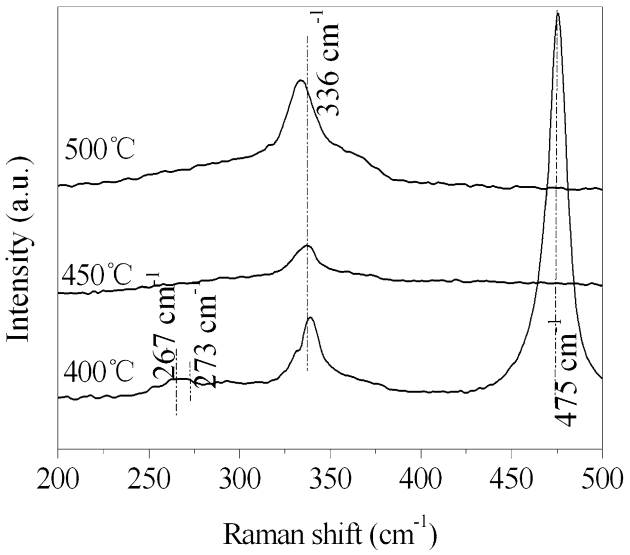

Fig. 4 Raman spectra of CZTS thin films at different temperatures

peak in all samples shifts slightly to lower wave number. It is attributed to the internal strain, which is caused by the shrinking of substrate during cooling down [29]. The presence of the internal strain is in good accordance with XRD analysis. Moreover, the deviation of wave number enhance with increasing the annealing temperature in all samples. So it is concluded that the internal strain is associated with the annealing temperature. The choice of proper cooling rate can reduce the internal strain.

3.3 Scanning electron micrograph

Figure 5 shows scanning electron micrograph images of the CZTS thin films at different temperatures. All samples are covered with grains with different sizes. For the CZTS thin film at 400 °C, the surface shows a poor crystalline quality with few voids and a grain size between 50 and 200 nm. The CZTS thin film at 450 °C exhibits irregularly shaped grains in the range of 100–400 nm. Larger agglomeration of grains in the CZTS thin film at 500 °C than those at 400 and 450 °C is identified, which is beneficial in photovoltaic application. It is concluded that a high annealing temperature can improve the crystallinity and grain sizes. We also investigate that the thickness of CZTS thin films at 400 °C, 450 °C and 500 °C are about 400 nm, 800 nm and 1 μm, respectively, showing that the thickness increases with increasing temperature due to grain growth, which further verify above conclusion. The results are consistent with the

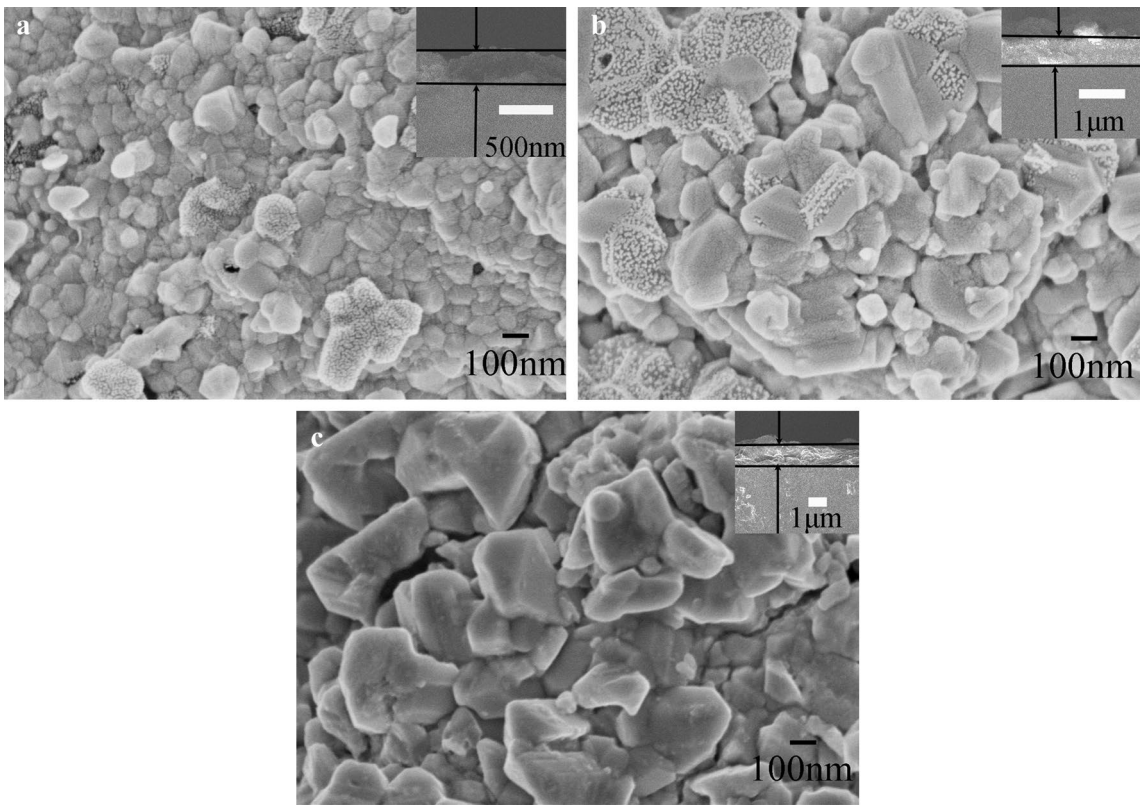

Fig. 5 SEM images of CZTS thin films at different temperatures **a** 400 °C, **b** 450 °C, **c** 500 °C. *Inset* The cross-section images of CZTS thin films at different temperatures **a** 400 °C, **b** 450 °C, **c** 500 °C

XRD patterns. In addition, some grains with rough surface in the samples at 400 and 450 °C can be clearly observed, whereas they are absent in the sample at 500 °C. Therefore, the ones were analyzed by SEM–EDX analysis where only neglected zinc in the areas was noted, indicating the existence of $Cu_{2-x}S$ and Cu_2SnS_3 phases for the grains with rough surface. It is probably due to the fact that the reaction is incompletely at 400 and 450 °C. So the proper sulfurization temperature is 500 °C.

3.4 Optical and electrical properties

The optical absorption coefficient versus the photo energy (as an inset) and optical bandgap estimations of the CZTS thin films at different temperatures are shown in Fig. 6. It can be seen that the annealed CZTS thin films exhibit a large optical absorption coefficient, which is larger than 10^4 cm^{-1} in the visible wavelength region. The optical absorption coefficient saturation for all films at a photon energy is close to 1.5 eV. The optical bandgap energies of the CZTS thin films annealed at different sulfurization temperatures are 1.42, 1.44 and 1.49 eV, respectively. The CZTS thin films annealed at 400 and 450 °C have relatively narrow bandgap energies due to the presence of $Cu_{2-x}S$ and Cu_2SnS_3 phases. It is concluded that the CZTS thin film at 500 °C is promising absorber material for thin-film solar cells due to its high absorption coefficient ($>10^4$ cm^{-1}) and optimal band gap (1.49 eV). The electrical properties of the CZTS thin film at 500 °C were also studied by Hall effect measurement at room temperature. The carrier concentration and mobility are about 3.652×10^{18} cm^{-3} and 26.32 cm^2/Vs, respectively.

4 Conclusion

In this paper, Cu_2ZnSnS_4 (CZTS) was prepared by sulfurizing Cu–Sn–Zn precursors deposited via a simple solution method. All CZTS thin films are Cu and Zn rich and Sn poor. XRD and Raman studies show that the crystal structure of CZTS thin film annealed at 500 °C is a single phase, whereas the ones annealed at 400 and 450 °C

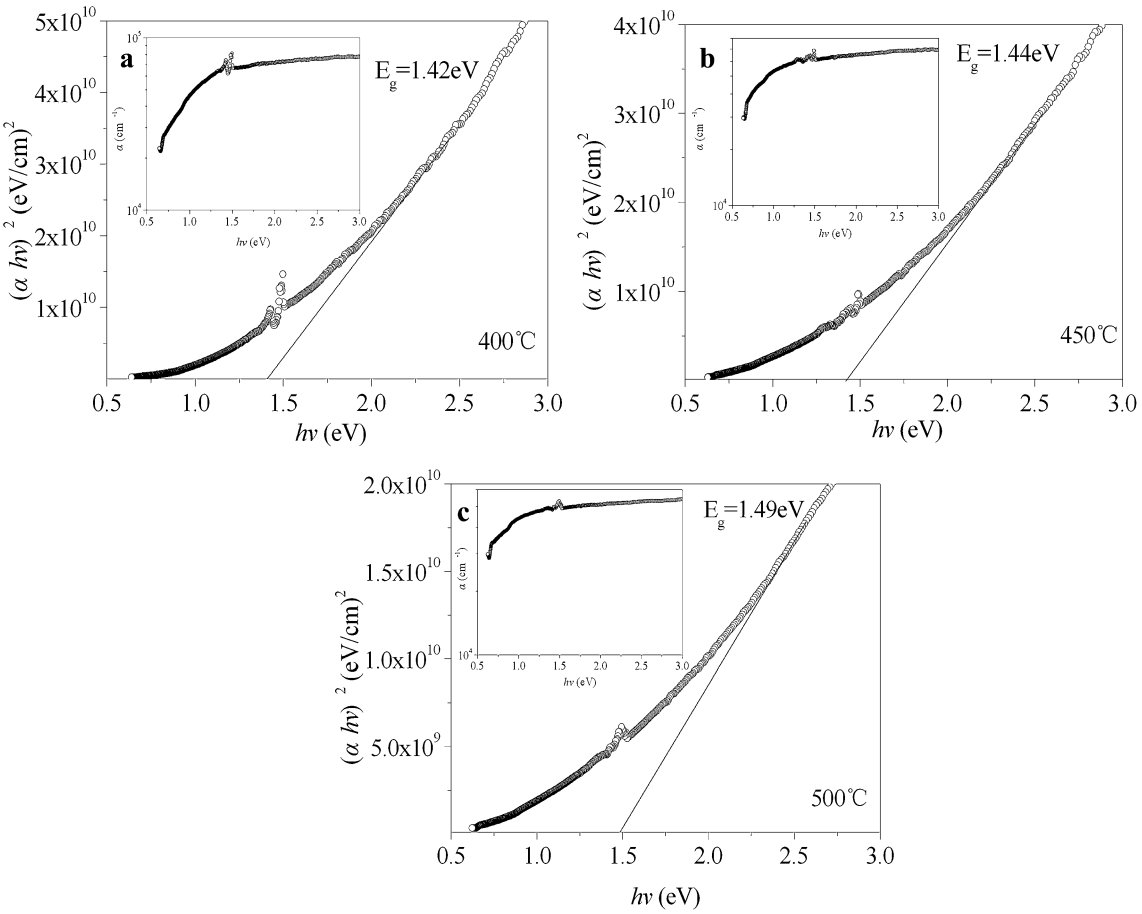

Fig. 6 Optical bandgap estimations of the CZTS thin films at different temperatures. *Inset* Optical absorption coefficient curve of the CZTS thin films at different temperatures

contain secondary phases such as $Cu_{2-x}S$, Cu_2SnS_3 and ZnS. The CZTS thin film annealed at 500 °C also shows the smallest micro-strain and dislocation density, indicating the sulfurization temperature is proper. From the scanning electron microscopy images, the CZTS thin film annealed at 500 °C shows the largest agglomeration of grains. Analysis of the optical and electrical properties reveals that the best CZTS thin film is the one annealed at 500 °C, exhibiting high absorption coefficient ($>10^4$ cm^{-1}), optimal band gap (1.49 eV), the carrier concentration (3.652×10^{18} cm^{-3}) and mobility (26.32 cm^2/Vs).

Acknowledgements This research is financial supported by National Science Foundation of China (61176062), Project of Jiangsu Industry-Academia-Research (BY2015057-19), the Priority Academic Program Development of Jiangsu Higher Education Institutions, Funding of Jiangsu Innovation Program for Graduate Education (CXLX12_0146), the research fund of Jiangsu Province Cultivation base for State Key Laboratory of Photovoltaic Science and Technology (SKLPSTKF201506) and the Fundamental Research Funds for the Central Universities.

References

1. K.W. Sun, C. Yan, F.Y. Liu, J.L. Huang, F.Z. Zhou, J.A. Stride, M. Green, X.J. Hao, Adv. Energy Mater. **6**, 1600046 (2016)
2. B. Shin, O. Gunawan, Y. Zhu, N.A. Bojarczuk, S.J. Chey, S. Guha, Prog. Photovolt. Res. Appl. **21**, 72 (2013)
3. C. Li, E. Ha, W. Wong, Z.C. Li, K. Ho, K. Wong, Mater. Res. Bull. **3201**, 47 (2012)
4. Y. Feng, T. Lau, G. Cheng, L. Yin, Z. Li, H. Luo, Z. Liu, X. Lu, C. Yang, X. Xiao, CrystEngComm **18**, 1070 (2016)
5. F.Y. Liu, Y. Li, K. Zhang, B. Wang, C. Yan, Y. H. Lai, Sol. Energy Mater. Sol. Cells 94, 2431 (2010)
6. H. Nozaki, T. Fukano, S. Ohta, Y. Seno, H. Katagiri, K. Jimbo, J. Alloys Compd. **524**, 22 (2012)
7. J. Li, H. shen, Y. Li, H. Yao, W. Wang, W. Wu, Z. Ren, J Mater. Sci. **27**(8), 8688 (2016)
8. M. Courel, E. Valencia-Resendiz, J.A. Andrade-Arvizu, E. Saucedo, O. Vigil-Galán, Sol. Energy Mater. Sol. Cells **159**, 151 (2016)
9. N.M. Shinde, R.J. Deokate, C.D. Lokhande, J. Anal. Appl. Pyrolysis **100**, 12 (2013)
10. B.A. Schubert, B. Marsen, S. Cinque, T. Unold, R. Klenk, S. Schoor, H.W. Schock, Prog. Photovolt. Res. Appl. **19**, 93 (2011)
11. R. Yu, T. Hung, Appl. Surf. Sci. **364**, 909 (2016)
12. R. Liu, M. Tan, X. Zhang, J. Chen, S. Song, W. Zhang, J. Alloys Compd. **655**, 124 (2016)
13. A. Tang, J. Liu, J. Ji, M. Dou, Z. Li, F. Wang, Appl. Surf. Sci. **383**, 253 (2016)
14. J. Tao, L. Chen, H. Cao, C. Zhang, J. Liu, Y. Zhang, L. Huang, J. Jiang, P. Yang, J. Chu, J. Mater. Chem. A **4**, 3798 (2016)
15. K.D. Lee, S.W. Seo, D.K. Lee, H. Kim, J.H. Jeong, M.J. Ko, B.S. Kim, D.H. Kim, J.Y. Kim, Thin Solid Films **546**, 294 (2013)
16. N.M. Shinde, D.P. Dubal, D.S. Dhawale, C.D. Lokhande, J.H. Kim, J.H. Moon, Mater. Res. Bull. **47**, 302 (2012)
17. S.S. Mali, P.S. Shinde, C.A. Betty, P.N. Bhosale, Y.W. Oh, P.S. Patil, J. Phys. Chem. Solid **73**, 735 (2012)
18. S.S. Mali, P.S. Shinde, C.A. Betty, P.N. Bhosale, Y.W. Oh, S.R. Jadkar, R.S. Devan, Y.R. Ma, P.S. Patil, Electrochim. Acta **66**, 216 (2012)
19. W. Wang, H. Shen, L.H. Wong, Z. Su, H. Yao, Y. Li, RSC Adv. **6**, 54049 (2016)
20. M. Zhou, Y. Gong, J. Xu, G. Fang, Q. Xu, J. Dong, J. Alloys Compd. **574**, 272 (2013)
21. A. Fischereder, T. Rath, W. Haas, H. Amenitsch, J. Albering, D. Meischler, S. Larissegger, M. Edler, R. Saf, F. Hofer, G. Trimmel, Chem. Mater. **22**, 3399 (2010)
22. A. Fischereder, A. Schenk, T. Rath, W. Haas, S. Delbos, C. Gougaud, N. Naghavi, A. Patater, R. Saf, D. Schenk, M. Edler, K. Bohnemann, A. Reichmann, B. Chernev, F. Hofer, G. Trimmel, Monatsh. Chem. **144**, 273 (2013)
23. Y. Guo, J. Wei, Y. Liu, T. Yang, Z. Xu, Nanoscale Res. Lett. **12**, 181 (2017)
24. X. Jin, J. Li, G. Chen, C. Xue, W. Liu, C. Zhu, Sol. Energy Mater. Sol. Cells **146**, 16 (2016)
25. F. Jiang, S. Ikeda, T. Harada, M. Matsumura, Adv. Energy Mater. **4**, 1301381 (2014)
26. R. Sathyamoorthy, C. Sharmila, K. Natarajan, S. Velumani, Mater. Charact. **58**, 745 (2007)
27. S. Kahraman, S. Çetinkaya, H.A. Çetinkara, H.S. Güder, Thin Solid Films **550**, 36 (2014)
28. H. Katagiri, N. Sasaguchi, S. Hando, S. Hoshino, J. Ohashi, T. Yokota, Sol. Energy Mater. Sol. Cells **49**, 407 (1997)
29. L. Sun, J. He, H. Kong, F.Y. Yue, P.X. Yang, J.H. Chu, Sol. Energy Mater. Sol. Cells **95**, 2907 (2011)